On-Line Aircraft Parameter Identification Using Fourier Transform Regression With an Application to NASA F/A-18 Harv Flight Data

Yongkyu Song*

School of Aerospace and Mechanical Engineering, Haukuk Aviation University,
Kyunggi-do 412-791, Korea

Byungheum Song

Department of Flight Operation, Hankuk Aviation University, Kyunggi-do 412-791, Korea

Brad Seanor, Marcello R. Napolitano

Department of Mechanical and Aerospace Engineering, West Virginia University, Morgantown,
WV 26506/6106, U.S.A.

This paper applies a recently developed on-line parameter identification (PID) technique to sets of real flight data and compares the results with those of a state-of-the-art off-line PID technique. The on-line PID technique takes Linear Regression from Fourier Transformed equations and the off-line PID is based on the traditional Maximum Likelihood method. Sets of flight data from the NASA F/A-18 High Alpha Research Vehicle (HARV) aircraft, which has been recorded from specifically designed maneuvers and used for off line parameter estimation, are used for this study. The emphasis is given on the accuracy and on-line measure of reliability of the estimates. The comparison is performed for both longitudinal and lateral-directional dynamics for maneuvers at angles of attack ranging $\alpha = 20°$ through $\alpha = 40°$. Results of the two estimation processes are also compared with baseline wind tunnel estimates whenever possible.

Key Words: On-line Parameter Identification, Fourier Tansform, Flight Data

Nomenclature

b	: Wing span, ft
$\bar{c}$	: Mean aerodynamic chord, ft
C_i	: Aerodynamic coefficient, 1/rad or 1/deg
g	: Gravity acceleration, ft/sec²
I	: Moment of inertia, slug/ft³
J	: Cost functional
k	: Numerical coefficient
m	: Aircraft mass, slug
p	: Roll rate, deg/sec
q	: Pitch rate, deg/sec
R	: Conversion from radian to degrees
$\bar{q}$	: Dynamic pressure, lbs/ft²
r	: Yaw rate, deg/sec
S	: Wing area, ft²
t	: Time, sec
T	: Thrust, lbs.
V	: Velocity, ft/sec
W	: Diagonal weighting matrix
Y	: Vector of known responses
X	: Matrix of known inputs

Greek

α	: Angle of attack, deg
β	: Sideslip angle, deg
Δ	: Incremental change
δ	: Control surface deflection, deg
∇	: Gradient
ζ	: Parameter vector to be estimated in ML

* Corresponding Author,
  E-mail : yksong@mail.hangkong.ac.kr
  TEL : +82-2-300-0115; FAX : +82-2-3158-2191
  School of Aerospace and Mechanical Engineering,
  Haukuk Aviation University Kyunggi-do 412-791,
  Korea. (Manuscript **Received** June 12, 2001; **Revised**
  December 12, 2001)

Θ : Parameter vector to be estimated in FTR

θ : Pitch angle, deg

ϕ : Roll angle, deg

Σ : Summation

Ψ : Yaw angle, deg

ω : Frequency, rad/sec

Subscripts

a : Aileron

D : Drag force

dht : Differential horizontal tail

e : Elevator

L : Lift force

l : Rolling moment

lef : Leading edge flap

m : Pitching moment

n : Yawing moment

o : Basic airframe

r : Rudder

sa : Symmetric aileron

tef : Trailing edge flap

$wind$: Wind axis

pv : Pitch vane

Y : Lateral force

yv : Yaw vane

Acronyms

CG : Center of Gravity

DOF : Degrees Of Freedom

DFT : Discrete Fourier Transform

$DFRC$: Dryden Flight Research Center

$DTFT$: Discrete Time Fourier Transform

EE : Estimation Error

FTR : Fourier Transform Regression

$HARV$: High Alpha Research Vehicle

LS : Least Squares

ML : Maximum Likelihood

NR : Newton–Raphson

$OBES$: On-Board Excitation System

PID : Parameter Identification

SVD : Singular Value Decomposition

1. Introduction

Traditionally parameter identification has been an important area to obtain a modeling of aircraft dynamics and examine the validity of design. The controller design and/or stability analysis has been performed usually with the identified system. For this purpose parameter identification has been performed off-line with measurements of outputs and inputs. Recent adaptive control or fault tolerant control, however, often tries to combine parameter identification and a good control scheme on-line to get best performance, thus requiring fast parameter identification scheme. In this context the speed of parameter convergence, reliability, and accuracy become key issues (Campa et al, 2001).

Especially the adaptive control with fast parameter identification has been pursuited in research aircraft programs such as the Reconfiguration Control for Tailless Fighter Aircraft (RESTORE) program (Brinker and Wise, 1999, Calise et al, 1998), the ACTIVE program, using a F-15 aircraft (Jorgensen, 1997), and the XV-15 program (tilt-rotor aircraft) (Rysdyk and Calise, 1998).

Like off-line parameter identification (PID) approaches, on-line PID methods can be formulated either in the time domain or in the frequency domain. Within time domain on-line PID techniques Least Squares (LS) based algorithms are used in lieu of gradient-based techniques because of their better convergence properties and lower computational effort. Therefore on-line time domain PID techniques mainly include variations of the LS method, such as Recursive Least Square (RLS) (Mendel, 1973, Ljung, 1987), RLS with a forgetting factor (Bodson, 1995), a Modified Sequential Least Square (MSLS) (Monaco et al, 1997), a real-time Batch Least Squares (BLS) (Chandler et al, 1995), and Extended Kalman Filtering (EKF) (Gelb et al, 1973). The real-time applications of any of these methods present substantial challenges because of the unavoidable presence of system and measurement noises, lack of information for PID purposes in the data, and potential unavailability of independent control inputs – a necessary condition for an accurate PID – especially due to the interactions with the closed-loop control laws. Analytical mechanisms to handle some of the above problems include the use of temporal and spatial constraints such as

forgetting factors. Another potential problem with time-domain PID techniques is the lack of a reliable measure for on-line assessment of the accuracy of the estimates in the presence of unmodeled noise.

The objective of this paper is to apply a recently developed Fourier Transform-based PID technique (Seanor et al, 2001, Morelli 1999) to NASA F/A-18 HARV flight data and compare the results with those of the application of the well-known Maximum Likelihood method, which is state-of-the-art off-line PID technique to date. The results from two approaches are then compared with the baseline wind tunnel estimates. The comparison is performed on both longitudinal and lateral-directional dynamics for maneuvers at angles of attack ranging $\alpha=20°$ through $\alpha=40°$.

This paper is organized as follows. The next section briefly describes the considered aircraft and the flight test maneuvers with relative data. The next section gives a linearization of the mathematical modeling of longitudinal and lateral-directional aircraft dynamics to apply the on-line PID technique. Another section reviews the basic principles of the well-known Maximum Likelihood method while the following section reviews the Fourier Transform Regression PID technique. The final section describes the results of the application of both methods using the F/A-18 HARV flight data.

2. Mathematical Modeling of the NASA F/A-18 HARV and Flight Test Maneuvers

The NASA F/A-18 HARV is a high alpha testbed aircraft which was used in the high alpha technology program at Dryden Flight Research Center. The HARV is from a pre-production model F/A-18 aircraft built by former McDonnell Douglas. Conventional control surfaces include stabilators, rudders, ailerons, leading-edge flaps, trailing-edge flaps and speed brake. An additional thrust vectoring system was added to the aircraft for the research purposes of the HARV program to increase the regime of

Table 1 Mass and geometric characteristics of the NASA F/A-18 HARV

Aircraft Weight (lbs)	36,099
CG Location (% m.a.c.)	23.8
I_x (slug-ft^2)	22,789
I_y (slug-ft^2)	176,809
I_z (slug-ft^2)	191,744
I_{xz} (slug-ft^2)	−2,305
Length (ft)	56
Wing Area (ft^2)	400
Wing Span (ft)	37.4
Wing Mean Aerodynamic Chord (ft)	11.52
Wing Aspect Ratio	3.5
Stabilator Total Span (ft)	21.6
Stabilator Total Area (ft^2)	86.48
Trailing Edge Flap Span (ft per wing)	8.72
Trailing Edge Flap Total Area (ft^2)	61.9
Leading Edge Flap Span (ft per wing)	13.8
Leading Edge Flap Total Area (ft^2)	48.4
Aileron Span (ft per wing)	5.68
Aileron Total Area (ft^2)	24.4
Rudder Span (ft per vertical tail)	5.21
Rudder Total Area (ft^2)	15.44

* All listed mass characteristics represent a 60% fuel load

stable flight up to $\alpha=70°$ and increase the aircraft maneuverability at high angles of attack. The three view of F/A-18 HARV is shown in Fig. 1 and the mass and geometric characteristics are listed in Table 1. The longitudinal and lateral-directional flight test maneuvers consisted of single surface independent control surface doublets generated by an on-board excitation system (OBES). The longitudinal flight data inputs consisted of trailing-edge flaps, symmetrically deflected ailerons, stabilator, and pitch vanes. Finally, the lateral-directional inputs consisted of ailerons, differential horizontal tail, rudder, and yaw vanes.

The aircraft dynamics are modeled in the body-axis equations of motion as follows:

$$m\ddot{x}_{cg} = T + C_X \bar{q} S - mg \sin \theta \qquad (1)$$
$$m\ddot{y}_{cg} = C_Y \bar{q} S + mg \sin \phi \cos \theta \qquad (2)$$
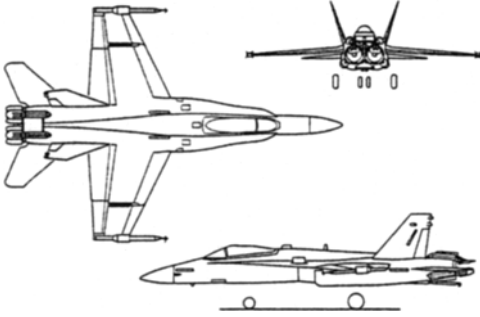$$m\ddot{z}_{cg} = C_Z \bar{q} S + mg \cos \phi \cos \theta \qquad (3)$$

Fig. 1 Three view of F/A-18 HARV

$$I_x\dot{p} - I_{xz}\dot{r} + (I_z - I_x)\,qr - I_{xz}pq = \bar{q}SbC_l \quad (4)$$

$$I_y\dot{q} + (I_x - I_z)\,rp + I_{xz}(p^2 - r^2)$$
$$= \bar{q}S\bar{c}C_m + (d_{TV} - x_{cg}) \cdot T \cdot C_{m_{\delta pv}}\delta p\nu \quad (5)$$

$$I_z\dot{r} - I_{xz}\dot{p} + (I_y - I_x)\,pq + I_{xz}qr$$
$$= \bar{q}SbC_n + (d_{TV} - x_{cg}) \cdot T \cdot C_{n_{\delta yv}}\delta y\nu \quad (6)$$

where T is the installed thrust and d_{TV} is the longitudinal distance of the location of the thrust vectoring vanes. The component build-up for the total longitudinal and lateral-directional stability and control derivatives is given by:

$$C_X = C_{X_0} + C_{X_\alpha}\alpha + C_{X_{\delta e}}\delta e + C_{X_{\delta lef}}\delta lef$$
$$+ C_{X_{\delta tef}}\delta tef + C_{X_{\delta sa}}\delta sa + C_{X_q}\left(\frac{\bar{c}}{2V}\right)q$$
$$+ \left(\frac{T}{\bar{q}S}\right)C_{X_{\delta pv}}\delta pv \quad (7)$$

$$C_Y = C_{Y_0} + C_{Y_\beta}\beta + C_{Y_{\delta a}}\delta a + C_{Y_{\delta r}}\delta r$$
$$+ C_{Y_{\delta dht}}\delta dht + C_{Y_p}\left(\frac{b}{2V}\right)p$$
$$+ C_{Y_r}\left(\frac{b}{2V}\right)r + \left(\frac{T}{\bar{q}S}\right)C_{Y_{\delta yv}}\delta yv \quad (8)$$

$$C_Z = C_{Z_0} + C_{Z_\alpha}\alpha + C_{Z_{\delta e}}\delta e + C_{Z_{\delta lef}}\delta lef$$
$$+ C_{Z_{\delta tef}}\delta tef + C_{Z_{\delta sa}}\delta sa + C_{Z_q}\left(\frac{\bar{c}}{2V}\right)q$$
$$+ \left(\frac{T}{\bar{q}S}\right)C_{Z_{\delta pv}}\delta pv \quad (9)$$

$$C_l = C_{l_0} + C_{l_\beta}\beta + C_{l_{\delta a}}\delta a + C_{l_{\delta r}}\delta r + C_{l_{\delta dht}}\delta dht$$
$$+ C_{l_p}\left(\frac{b}{2V}\right)p + C_{l_r}\left(\frac{b}{2V}\right)r \quad (10)$$

$$C_m = C_{m_0} + C_{m_\alpha}\alpha + C_{m_{\delta e}}\delta e + C_{m_{\delta lef}}\delta lef$$
$$+ C_{m_{\delta tef}}\delta tef + C_{m_{\delta sa}}\delta sa + C_{m_q}\left(\frac{\bar{c}}{2V}\right)q \quad (11)$$
$$+ \left(\frac{d_{TV} - x_{cg}}{\bar{c}}\right)\left(\frac{T}{\bar{q}S}\right)C_{m_{\delta pv}}\delta pv$$

$$C_n = C_{n_0} + C_{n_\beta}\beta + C_{n_{\delta a}}\delta a + C_{n_{\delta r}}\delta r + C_{n_{\delta dht}}\delta dht$$

$$+ C_{n_p}\left(\frac{b}{2V}\right)p + C_{n_r}\left(\frac{b}{2V}\right)r$$
$$+ \left(\frac{d_{TV} - x_{cg}}{b}\right)\left(\frac{T}{\bar{q}S}\right)C_{n_{\delta yv}}\delta yv \quad (12)$$

The measurements of the accelerations at the center of gravity are related to the measurements at different locations using the relationships:

$$\ddot{x}_{cg} = a_X + (x_{cg} - x_{ax})\,(q^2 + r^2) + (y_{ax} - y_{cg})$$
$$(\dot{r} - qp) - (z_{cg} - z_{ax})\,(q + rp) \quad (13)$$

$$\ddot{y}_{cg} = a_Y - (x_{cg} - x_{ay})\,(\dot{r} + pq) + (y_{ay} - y_{cg})$$
$$(r^2 + p^2) + (z_{cg} - z_{ay})\,(\dot{p} - rq) \quad (14)$$

$$\ddot{z}_{cg} = a_Z + (x_{cg} - x_{az})\,(\dot{q} - pr) - (y_{az} - y_{cg})$$
$$(\dot{p} + qr) + (z_{cg} - z_{az})\,(q^2 + p^2) \quad (15)$$

where $x_{ai}, y_{ai}, z_{ai}\,(i = x, y, z)$ are the coordinates of the location of the i-th accelerometer on the aircraft. For later use the NASA F/A-18 HARV dynamics are linearized through small-perturbation theory using $T = T_0 + \Delta T$, $a_x = a_{x_0} + \Delta a_x$, etc., as follows :

$$\Delta T - m\{\Delta a_x - (z_{cg} - z_{az})\Delta\dot{q} + (y_{az} - y_{cg})\Delta\dot{r}\}$$
$$= \bar{q}S\{C_{X_\alpha}\Delta\alpha + C_{X_{\delta e}}\Delta\delta e + C_{X_{\delta lef}}\Delta\delta lef$$
$$+ C_{X_{\delta tef}}\Delta\delta tef + C_{X_{\delta sa}}\Delta\delta sa + C_{X_q}\left(\frac{\bar{c}}{2V}\right)\Delta q$$
$$+ \left(\frac{T_0}{\bar{q}S}\right)C_{X_{\delta pv}}\Delta\delta pv \quad (16)$$

$$m\{\Delta a_Y - (x_{cg} - x_{ay})\Delta\dot{r} + (z_{cg} - z_{ay})\Delta\dot{p}\}$$
$$= \bar{q}S\{C_{Y_\beta}\Delta\beta + C_{Y_{\delta a}}\Delta\delta a + C_{Y_{\delta r}}\Delta\delta r$$
$$+ C_{Y_{\delta dht}}\Delta\delta dht + C_{Y_p}\left(\frac{b}{2V_0}\right)\Delta p$$
$$+ C_{Y_r}\left(\frac{b}{2V_0}\right)\Delta r + \left(\frac{T_0}{\bar{q}S}\right)C_{Y_{\delta yv}}\Delta\delta yv\} \quad (17)$$

$$m\{\Delta a_z + (x_{cg} - x_{az})\Delta\dot{q} - (y_{az} - y_{cg})\Delta\dot{p}\}$$
$$= \bar{q}S\{C_{Z_\alpha}\Delta\alpha + C_{Z_{\delta e}}\Delta\delta e + C_{Z_{\delta lef}}\Delta\delta lef + C_{Z_{\delta tef}}\Delta\delta tef$$
$$+ C_{Z_{\delta sa}}\Delta\delta sa + C_{Z_q}\left(\frac{\bar{c}}{2V}\right)\Delta q + \left(\frac{T_0}{\bar{q}S}\right)C_{Z_{\delta pv}}\Delta\delta pv \quad (18)$$

$$I_x\Delta\dot{p} - I_{xz}\Delta\dot{r} = \bar{q}Sb\{C_{l_\beta}\Delta\beta + C_{l_{\delta a}}\Delta\delta a + C_{l_{\delta r}}\Delta\delta r$$
$$+ C_{l_{\delta dht}}\Delta\delta dht + C_{l_p}\left(\frac{b}{2V_0}\right)\Delta p + C_{l_r}\left(\frac{b}{2V_0}\right)\Delta r\} \quad (19)$$

$$I_y\Delta\dot{q} = \bar{q}S\bar{c}\{C_{m_\alpha}\Delta\alpha + C_{m_{\delta e}}\Delta\delta e + C_{m_{\delta lef}}\Delta\delta lef$$
$$+ C_{m_{\delta tef}}\Delta\delta tef + C_{m_{\delta sa}}\Delta\delta sa + C_{m_q}\left(\frac{\bar{c}}{2V_0}\right)\Delta q\}$$
$$+ (d_{TV} - x_{cg}) \cdot T_0 \cdot C_{m_{\delta pv}}\Delta\delta pv \quad (20)$$

$$I_z\Delta\dot{r} - I_{xz}\Delta\dot{p} = \bar{q}Sb\{C_{n_\beta}\Delta\beta + C_{n_{\delta a}}\Delta\delta a$$
$$+ C_{n_{\delta r}}\Delta\delta r + C_{n_{\delta dht}}\Delta\delta dht + C_{n_p}\left(\frac{b}{2V_0}\right)\Delta p$$

$$+ C_{nr} \Big(\frac{b}{2V_0} \Big) \Delta r + \Big(\frac{d_{IV} - x_{cg}}{b} \Big) \Big(\frac{T_0}{\bar{q}S} \Big) C_{n_{\delta y v}} \Delta \delta y v \} \quad (21)$$

3. Review of the Maximum-Likelihood Method with Newton-Raphson Technique

In this section we briefly review the Maximum Likelihood method and the reader may refer to Maine and Iliff, 1985 for detail. The Maximum Likelihood (ML) method coupled with a Newton-Raphson (NR) minimization technique has been one of the most successful PID methods for several years. It was introduced at NASA Dryden in the late 1960's. The effectiveness of this approach is well documented and excellent results have been achieved for a large variety of aircraft. This method minimizes a quadratic cost function containing differences between the aircraft measured and computed responses. In general, the goal is to maximize the probability that the computed system responses, based on a set of estimated stability derivatives, are representative of the true system dynamics. Using the maximum likelihood method the conditional probability to be maximized is given by:

$$P(z) = P(z/\xi) P(\xi)$$
$$= \frac{1}{2\pi^{\big(\frac{n_t n_z + n_t}{2} \big)} \Big(\frac{1}{W_1} \Big)^{\frac{n_t}{2}} \Big(\frac{1}{W_2} \Big)^{\frac{1}{2}}} e^{-\frac{1}{2} J(\xi)} \quad (22)$$

where $P(z/\xi)$ and $P(\xi)$ are given by:

$$P(z/\xi) = \frac{1}{2\pi^{(n_t n_z)} \mid W_1^{-1} \mid^{\frac{n_z}{2}}} e^{-J(\xi)} \quad (23)$$

$$P(\xi) = \frac{1}{2\pi^{(n_{\xi/2})} \mid w_2^{-1} \mid^{\frac{1}{2}}} e^{-\frac{1}{2}[(\xi - \xi_0)^T W_2(\xi - \xi_0)]} \quad (24)$$

thus the problem reduces itself to the minimization of the cost function $J(\xi)$ given by:

$$J(\xi) = \frac{1}{2n_t n_z} \sum_{k=1}^{n_t} ([z(t_k) - y(t_k)]^T$$
$$W_1[z(t_k) - y(t_k)]) \quad (25)$$

In particular, $P(z/\xi)$ is the conditional probability that a response z occurs for an actual system for a given value of the unknown parameters contained in a vector ξ. $P(\xi)$ is the probability that the unknown parameters vector

matches some "a priori" values (ξ_0). It is assumed that $P(z/\xi)$ and $P(\xi)$ are independent and follow Gaussian distributions with zero means. The accuracy of the estimates increases as the differences between the values of the components of z and y, at the same discrete time index, decrease.

A Newton-Raphson (NR) algorithm is used to solve the associated system of equations by using the first and the second gradients of the cost function with respect to the vector (ξ) containing the aerodynamic parameters to be estimated. The relations for the NR algorithm can be discussed as the following.

The process is iterative with the updating of the vector ξ until the convergence criteria is met resulting in the final ML estimates of the aircraft model parameters. First a Taylor series expansion is used to generate an expression for $J(\xi)$, as is shown below:

$$J(\xi) = J(\xi_i) + \nabla_\xi J(\xi_i) \cdot (\Delta \xi)$$
$$+ \frac{1}{2} (\Delta \xi^T) \nabla_\xi^2 J(\xi_i) \cdot (\Delta \xi) \quad (26)$$

The NR algorithm solves the associated system of equations using the gradient and the hessian of the cost function with respect to the vector containing the aerodynamic parameters to be estimated. Setting the gradient with respect to ξ, equal to zero the cost function is minimized using:

$$\nabla_\xi J(\xi) = \bar{0} = \nabla_\xi J(\xi_i) + \nabla_\xi(\nabla_\xi J(\xi_i) \cdot (\Delta \xi))$$
$$+ \frac{1}{2} \nabla_\xi((\Delta \xi^T) \nabla_\xi^2 J(\xi_i) \cdot (\Delta \xi)) \quad (27)$$

$$\nabla_\xi^2 J(\xi_i) = \frac{1}{n_t n_z} \sum_{k=1}^{n_t} [[\nabla_\xi y(t_k)]^T W_1 \nabla_\xi y(t_k)] \quad (28)$$

leading to:

$$\xi_{i+1} = \xi_i - [(\nabla_\xi^2 J(\xi_i))]^{-1} \nabla_\xi J(\xi_i) \quad (29)$$

The process is iterative with the updating of the parameter vector ξ until the convergence criteria is met resulting in the final ML estimates of the aircraft model parameters.

4. On-line PID Using Fourier Transform Regression (FTR)

In this section a fast on-line PID method is modified and applied to get aerodynamic

coefficients for NASA F/A-18 HARV. The on-line PID method, which is called Fourier Transform Regression (Seanor et al, 2001), is a frequency-based simple single-step technique based on Discrete Time Fourier Transform (DTFT) using previous work described in (Morelli, 1999, Seanor et al, 2001). Consider a dynamic equation which is given in the form

$$A\dot{y}(t) + Bz(t) = x(t)^T \Theta \qquad (30)$$

where A, B are known constant vectors and Θ is an unknown constant vector to be estimated. Note that the linearized Eqs. (16)-(21) are in the form of (30). For example, in Eq. (16), we would have:

$$x = [\Delta a, \Delta q, \Delta \delta ef, \Delta \delta tef, \Delta \delta sa, \Delta \delta pve]^T$$
$$y = [\Delta q, \Delta r]^T$$
$$z = [\Delta T, \Delta a_x]^T$$

Sampling the input and motion variables at time $t = k\Delta t$ we have:

$$A\dot{y}(k\Delta t) + Bz(k\Delta t) = x(k\Delta t)^T \Theta \qquad (31)$$

Applying the Discrete Time Fourier Transform (DTFT) (Haykin and Van Veen, 1999) to the above samples we have:

$$Aj\omega\tilde{y}(\omega) + B\tilde{z}(\omega) = \tilde{x}(\omega)^T \Theta \qquad (32)$$

where

$$\tilde{x}(\omega) = \sum_{k=1}^{N-1} x(k\Delta t) e^{-j\omega k\Delta t}$$

$$\tilde{y}(\omega) = \sum_{k=0}^{N-1} y(k\Delta t) e^{-j\omega k\Delta t}$$

$$\tilde{z}(\omega) = \sum_{k=0}^{N-1} z(k\Delta t) e^{-j\omega k\Delta t} \qquad (33)$$

As in the general LS regression method, the measurements of the vectors x, y, and z can be used to set up a cost function having the aerodynamic coefficients as an argument. In particular, one can form the m algebraic equations which hold over a set of frequency points $[\omega_1, \omega_2, \cdots, \omega_m]$:

$$\begin{bmatrix} Aj\omega_1\tilde{y}(\omega_1) + B\tilde{z}(\omega_1) \\ Aj\omega_2\tilde{y}(\omega_2) + B\tilde{z}(\omega_2) \\ \cdots \\ \cdots \\ Aj\omega_m\tilde{y}(\omega_m) + B\tilde{z}(\omega_m) \end{bmatrix} = \begin{bmatrix} \tilde{x}^T(\omega_1) \\ \tilde{x}^T(\omega_2) \\ \cdots \\ \cdots \\ \tilde{x}^T(\omega_m) \end{bmatrix} \Theta \qquad (34)$$

Introducing a complex error vector ε, which

accounts for noise and non-linearities, the above equations can be rewritten in the general form $Y = X\Theta + \varepsilon$ with conventional definitions for Y, X, and Θ. Thus the problem can be formulated as a LS regression problem with the following complex cost function:

$$J = \frac{1}{2}(Y - X\Theta)^*(Y - X\Theta) \qquad (35)$$

The solution is given by:

$$\hat{\Theta} = [Re(X^*X)]^{-1}Re(X^*Y) \qquad (36)$$

where * indicates a complex conjugate transpose. Note that the cost function is made of a summation over m frequencies of interest. In addition, the covariance matrix of the estimates of $\hat{\Theta}$ is computed as

$$cov(\hat{\Theta}) = E\{(\hat{\Theta} - \Theta)(\hat{\Theta} - \Theta)^*\}$$
$$= \sigma^2(\hat{\Theta}) \cdot [Re(X^*X)]^{-1} \qquad (37)$$

where $\sigma^2(\hat{\Theta})$ is the equation error variance and can be estimated on-line using

$$\tilde{\sigma}^2(\hat{\Theta}) = \frac{1}{(m-p)}[(Y - X\hat{\Theta})^*(Y - X\hat{\Theta})] \qquad (38)$$

where p is the number of parameters to be estimated and m is the number of frequency points. Furthermore, the standard deviation of the estimation error for the l-th unknown of the p parameters in $\hat{\Theta}$ can be evaluated as the square root of the (l, l) coefficient (main-diagonal coefficient) of the covariance matrix. This standard deviation allows for an on-line assessment of the accuracy of the estimates of the parameter.

The type of required on-line calculations should also be analyzed for an assessment of the computational effort. For a given frequency, ω_n, the DTFT at the i-th time step is related to the DTFT at the $(i-1)$-th time step as follows:

$$\tilde{x}_k(\omega_n) = \tilde{x}_{k-1}(\omega_n) + x_k e^{-j\omega_n k\Delta t} \qquad (39)$$

Therefore, the on-line computation of $\tilde{x}_k(\omega_n)$ requires a reasonably low computational effort. In addition, the scheme requires only a fixed memory space for $\tilde{x}_k(\omega)$ even if it is updated at every step. Furthermore, a very important characteristic of this technique is that the time domain data from previous flight maneuvers-containing good information for PID purposes-

Table 2 Comparison of estimates for longitudinal aerodynamic coefficients

Aerodynamic Coefficients	$\alpha=30$ deg, M=0.38, h=37,822 ft			$\alpha=40$ deg, M=0.32, h=34,134 ft		
	WT	ML	FT (Std. Err.)	WT	ML	FT (Std. Err.)
C_{L_α}	–	0.0299	0.0362 (0.0023)	–	-0.0211	-0.0160 (0.0048)
C_{L_q}	4.5701	26.5462	61.8914 (7.9230)	-8.7421	-30.2781	-46.3713 (17.8646)
$C_{L_{\delta e}}$	0.0110	0.0100	0.0110 (0.0017)	-0.0089	-0.0076	-0.0110 (0.0043)
$C_{L_{\delta tef}}$	0.0068	0.0025	0.0066 (0.0006)	-0.0034	-0.0003	-0.00047 (0.00099)
$C_{L_{\delta sa}}$	0.0045	0.0022	0.0022 (0.0004)	-0.0008	-0.0016	-0.0016 (0.0008)
$C_{L_{\delta pv}}$	–	0.0110	0.0074 (0.0058)	–	-0.0102	-0.0293 (0.0171)
C_{m_α}	–	-0.0029	-0.0010 (0.0014)	–	-0.0058	-0.0058 (0.0017)
C_{m_q}	-6.0000	-12.2215	-10.7668 (4.7498)	-13.00	-11.6445	-13.4954 (6.2015)
$C_{m_{\delta e}}$	-0.0150	-0.0128	-0.0133 (0.0010)	-0.0120	-0.0106	-0.0117 (0.0015)
$C_{m_{\delta tef}}$	0.0013	0.0008	0.0015 (0.0004)	0.0016	0.0009	0.00055 (0.00034)
$C_{m_{\delta sa}}$	-0.0020	-0.0007	-0.0012 (0.0003)	-0.0013	-0.0007	-0.00077 (0.00027)
$C_{m_{\delta pv}}$	–	-0.0098	-0.0222 (0.0019)	–	-0.0103	-0.0181 (0.0031)
No. of MATLAB flops	–	–	13,734,909	–	–	13,743,187
MATLAB CPU Time	–	–	2.860 sec	–	–	3.350 sec

can still be used by simply iterating the calculation of the DTFT. Thus, the DTFT approach allows for retaining all the PID results from previous time steps and, at the same time, provides the necessary flexibility to follow changes in the system dynamics.

In terms of frequency range, the m frequencies over which the cost function is evaluated can be selected as evenly spaced between ω_{min} and ω_{max}. Typically, the rigid body dynamics frequency range for the considered aircraft can be selected allowing to filter out higher frequency noise and/

or structural interference. Clearly, a smaller range of frequency would decrease the computational effort.

Since the DTFT is recursively computed, the part of the algorithm requiring most computational effort is the inversion of matrix $\text{Re}(X^T X)$ which is performed using Singular Value Decomposition (SVD). Particularly, for each vector Θ of parameters to be estimated, one SVD ($O(n^3)$ flops) of the matrix $\text{Re}(X^T X)$ (average size 6 by 6) has to be performed for each computational step.

Table 3 Comparison of estimates for lateral/directional aerodynamic coefficients

Aerodynamic Coefficients	$\alpha=20$ deg			$\alpha=30$ deg		
	WT	ML	FT (Std. Err.)	WT	ML	FT (Std. Err.)
C_{Y_β}	-	-0.0116	-0.0021 (0.0024)	-	-0.0117	0.0006 (0.0024)
$C_{Y_{\delta A}}$	-0.0008	-0.73E-4	-0.0037 (0.0013)	0.0008	0.00055	-0.0031 (0.0016)
$C_{Y_{\delta R}}$	0.0028	0.0029	0.0012 (0.0008)	0.0019	0.0020	0.0012 (0.0009)
$C_{Y_{\delta dht}}$	-0.0001	0.000065	-0.0045 (0.0023)	0.0010	0.0021	-0.0048 (0.0027)
$C_{Y_{\delta yv}}$	-	0.0096	0.0032 (0.0042)	-	0.0125	0.0005 (0.0042)
C_{l_β}	-	-0.00335	-0.0031 (0.0002)	-	-0.0030	-0.0023 (0.0001)
C_{l_p}	-0.2300	-0.2617	-0.2839 (0.0658)	-0.4500	-0.2310	-0.2713 (0.0471)
$C_{l_{\delta A}}$	0.0013	0.0014	0.0011 (0.0001)	1.000E-3	1.0060E-3	0.8988E-3 (0.075E-3)
$C_{l_{\delta R}}$	0.00043	0.00016	0.7882E-4 (0.732E-4)	0.430E-3	0.2496E-3	0.1245E-3 (0.051E-3)
$C_{l_{\delta dht}}$	0.0006	0.00112	0.0016 (0.0002)	0.00065	0.0010	0.0011 (0.0001)
C_{n_β}	-	0.00095	0.0013 (0.0004)	-	0.4156E-3	0.5360E-3 (0.174E-3)
C_{n_r}	-	-0.2345	-0.7168 (0.3803)	-	-0.2778	-0.0634 (0.1484)
$C_{n_{\delta A}}$	-0.350E-3	-0.0732E-3	-0.0860E-3 (0.185E-3)	-0.400E-3	-0.2634E-3	-0.1820E-3 (0.109E-3)
$C_{n_{\delta R}}$	-0.0010	-0.00091	-0.0010 (0.0001)	-0.550E-3	-0.7108E-3	-0.6680E-3 (0.068E-3)
$C_{n_{\delta dht}}$	-0.004E-3	-0.4915E-3	-0.3678E-3 (0.331E-3)	-0.0002	-0.0010	-0.00072 (0.00018)
$C_{n_{\delta yv}}$	-	-0.0086	-0.0205 (0.0010)	-	-0.0094	-0.0186 (0.0005)
No. of MATLAB flops	-	-	34,039,134	-	-	34,038,034
MATLAB CPU Time	-	-	2.580 sec	-	-	2.520 sec

5. Results of the Comparative Study

The estimation results are summarized in Tab-les 2 and 3 for the longitudinal and lateral-directional maneuvers respectively. For the longitudinal maneuver at $\alpha=30°$, two longit-udinal time histories are shown in Fig. 2 with the
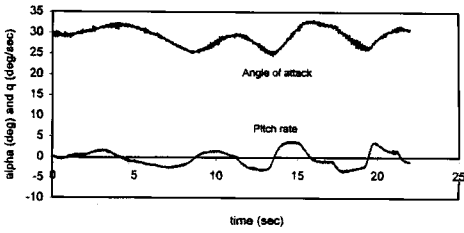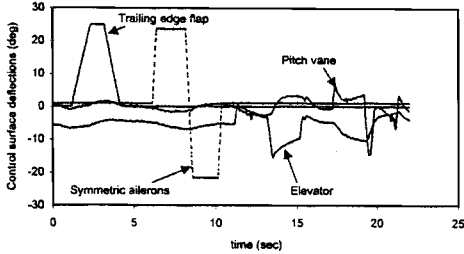
Fig. 2 Time histories of the longitudinal maneuver
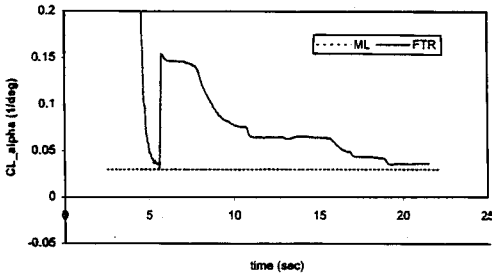

Fig. 3 Time histories of the longitudinal control inputs
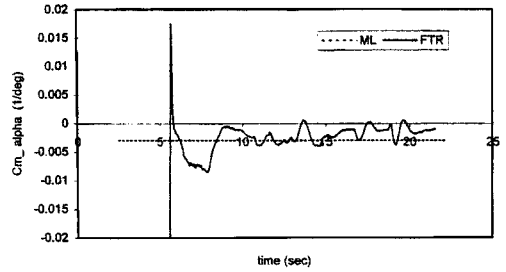

Fig. 4 Time history of C_{L_α} estimate

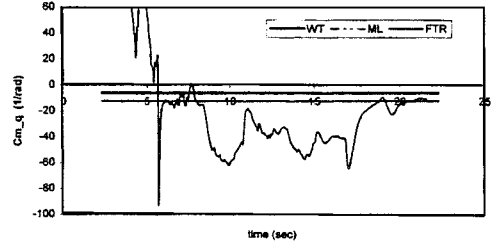

Fig. 5 Time history of C_{m_α} estimate

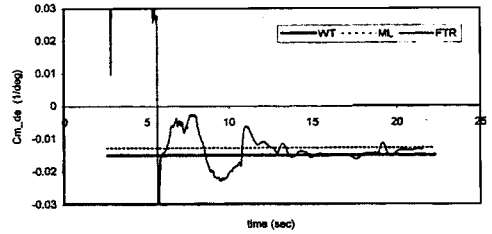

Fig. 6 Time history of C_{m_q} estimate

Fig. 7 Time history of $C_{m_{\delta e}}$ estimate

longitudinal inputs shown in Fig. 3. The time histories of the estimates for the longitudinal derivatives along with the relative maximum likelihood and wind tunnel estimates are shown in Figs. 4-7. It is seen that all the parameters were estimated within reasonable ranges and is comparable with both wind tunnel and off-line Maximum Likelihood results. It should also be noted that most of the standard deviation of the estimation errors are small except for the q-parameters, which are usually difficult to estimate from the flight data since they are coupled with the α-parameters.

For the lateral-directional maneuver at $\alpha = 30°$, several lateral-directional time histories are shown in Fig. 8 with the lateral-directional PID inputs shown in Fig. 9. The time histories of the estimates of the lateral-directional derivatives along with the relative maximum likelihood and wind tunnel estimates are shown in Figs. 10-13. In general the lateral-directional estimates seem to show more consistency between the results from the different methods. It is reminded that the estimation is performed sequentially as the flight data is received while most techniques including Maximum Likelihood method are executed in a post-processing batch mode. It can also be noted that derivatives converge within a short amount of time following the PID maneuver and the required computational times are very small (2.5-3.4 seconds for 22-29 second maneuvers). This convergence speed along with the computational
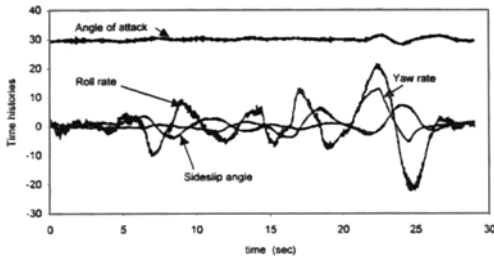
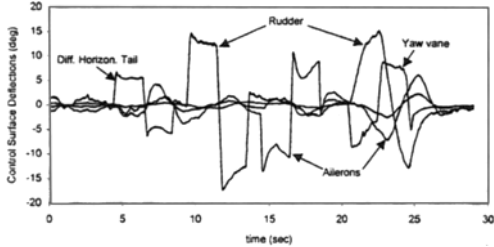**Fig. 8**   Time history of the lateral/directional maneuver

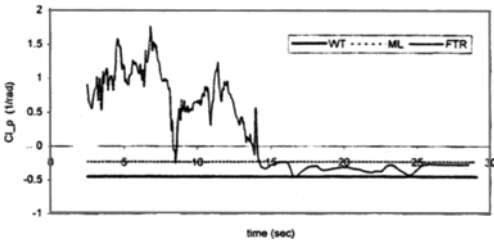**Fig. 9**   Time history of the lateral/directional control inputs
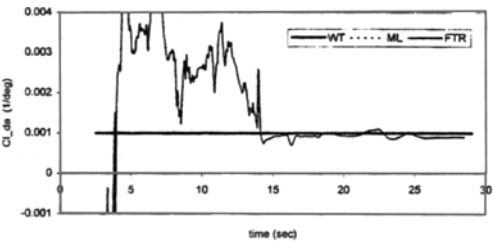

Fig. 10   Time history of C_{l_p} estimate

Fig. 11   Time history of $C_{l_{\delta A}}$ estimate

Fig. 12   Time history of C_{n_β} estimate

Fig. 13   Time history of $C_{n_{\delta R}}$ estimate

this technique provides totally independent reference values to parameters.

Conclusions

This paper has presented estimates for both longitudinal and lateral-directional derivatives from F/A-18 HARV flight data using Fourier Transform Regression (FTR) PID method. The estimation results have been compared with those by the state-of-the art off-line PID method, the well-known Maximum Likelihood approach coupled with a Newton-Raphson technique. It was seen that the FTR PID method provides very good estimates with small amount of computation time and quick convergence, and also gives good measure of reliability of the estimates on-line. These specific characteristics of the FTR-based PID method make it appealing for use with real time applications.

Acknowledgement

efficiency would make this technique appealing for applications within adaptive flight control systems. Another point to be noticed is that this technique does not use any "a priori" values of parameters and thus does not require any regularization with "a priori" values. Therefore,
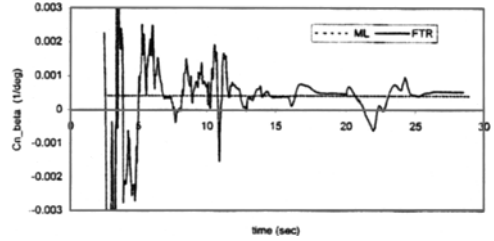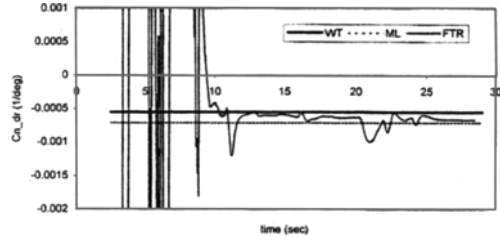
References

Bodson, M., 1995, "An Information-Dependent Data Forgetting Adaptive Algorithm," *Proceedings of the 1995 American Control Conference*, Seattle, WA.

Brinker, J. S., Wise, K. A., 1999, "Nonlinear Simulation Analysis of a Tailless Advanced Fighter Aircraft Reconfigurable Flight Control Law," *Proceedings of the 1999 AIAA Guidance Navigation and Control Conference*, AIAA Paper 99-4040, Portland, OR.

Campa, G., Fravolini, M. L., Song, Y., Napolitano, M., Seanor, B., 2001, "Application of an improved LWR Method to On-Line Aircraft Parameter Estimation Problems," *To be presented at 2001 IFAC Symposium on Automatic Control in Aerospace*, Bologna, Italy.

Calise, A. J., Lee, S., Sharma, M., 1998, "Direct Adpative Reconfigurable Control of a Tailless Fighter Aircraft," *Proceedings of the 1998 AIAA Guidance Navigation and Control Conference*, AIAA Paper 98-4108, Boston, MA.

Chandler, P., Patcher, M., Mears, M., 1995, "System Identification for Adaptive and Reconfigurable Control," *AIAA Journal of Guidance, Control and Dynamics*, Vol. 18, No. 3, pp. 516~524.

Gelb, A. et al., 1973, Applied Optimal Estimation, *MIT Press, Cambridge, Ma, 1973.*

Hoak, D. E. and Finck, R. D., 1978, *USAF Stability and Control DATCOM*, AFWAL-TR -83-3048.

Haykin S. and Van Veen, B., 1999, *Signals and Systems*, John Wiley and Sons, Inc.

Jorgensen, C. C., 1997, "Direct Adaptive Aircraft Control Using Dynamic Cell Structure Neural Networks," *NASA TM* 112198.

Klein, V., 1978, "Aircraft Parameter Estimation in Frequency Domain," *Proceedings of the 1978 AIAA Atmospheric Flight Mechanics Conference*, AIAA paper 78-1344, Palo Alto, CA.

Ljung, L., 1987, *System Identification : Theory for the User*, Prentice Hall, Englewood Cliffs, NJ.

Maine, R. E., Iliff, K. W., 1985, *Identification of Dynamic Systems: Theory and Formulation*, NASA RP-1138.

Mendel, J. M., 1973, *Discrete Techniques of Parameter Estimation*, Marcel Dekker, New York, NY.

Morelli, E. A., 1997, "High Accuracy Evaluation of the Finite Fourier Transform Using Sampled Data," *NASA TM* 110340.

Morelli, E. A., 1998, "In Flight System Identification," *Proceedings of the 1998 AIAA Atmospheric Flight Mechanics Conference*, AIAA paper 98-4261, Boston, MA.

Morelli, E. A., 1999, "Real-Time Parameter Estimation in the Frequency Domain," *Proceedings of the 1999 AIAA Atmospheric Flight Mechanics Conference*, AIAA paper 99-4043, Portland, OR.

Napolitano, M., An, Y., and Seanor, B. A., "A fault tolerant flight control system for sensor and actuator failures using neural networks," *Aircraft Design*, Vol. 3, pp. 103~128.

Neter, J., Kutner, M. H., Nachtsheim, C. J., and Wasserman, W., 1996, *Applied Linear Regression Models*, 3rd Ed. , Richard D. Irwin, Inc. , Burr Ridge, IL.

Roskam, J., 1994, *Airplane Flight Dynamics and Automatic Flight Controls: Part I*, Roskam Aviation and Engineering Coorporation, Ottawa, KA.

Rysdyk, R., Calise, A. J., 1998, "Fault Tolerant Flight Control Via Adaptive Neural Network Augmentation," *Proceedings of the 1998 AIAA Guidance Navigation and Control Conference*, AIAA Paper 98-4483, Boston, MA.

Seanor, B., Song, Y., Napolitano, M. R., and Campa, G., 2001, "Comparison of on-Line and Off-line Parameter Estimation Techniques Using the NASA F/A-18 HARV Flight Data," To be presented at 2001 AIAA Atmospheric Flight Mechanics Conference, AIAA Paper No. 2001 -4261.